Earth and Planetary Science Letters 422 (2015) 150–156

Contents lists available at ScienceDirect

Earth and Planetary Science Letters

www.elsevier.com/locate/epsl

Interannual variation of the Antarctic Ice Sheet from a combined analysis of satellite gravimetry and altimetry data

A. Mémin[a,b,*], T. Flament[c], B. Alizier[b], C. Watson[d], F. Rémy[c]

[a] Université Nice Sophia Antipolis, CNRS, IRD, Observatoire de la Côte d'Azur, Géoazur, UMR 7329, 250 rue Albert Einstein, Sophia Antipolis, 06560 Valbonne, France
[b] School of Physical Sciences, University of Tasmania, Private bag 37, TAS 7001, Hobart, Australia
[c] LEGOS/UMR 5566, Université Paul Sabatier/OMP, CNRS, 14 rue Edouard Belin, 31400 Toulouse, France
[d] School of Land and Food, University of Tasmania, Private bag 76, TAS 7001, Hobart, Australia

ARTICLE INFO

Article history:
Received 13 October 2014
Received in revised form 20 March 2015
Accepted 26 March 2015
Available online xxxx
Editor: P. Shearer

Keywords:
Antarctica
ice sheet
interannual variation
mass changes
GRACE
Envisat

ABSTRACT

Assessment of the long term mass balance of the Antarctic Ice Sheet, and thus the determination of its contribution to sea level rise, requires an understanding of interannual variability and associated causal mechanisms. We performed a combined analysis of surface-mass and elevation changes using data from the GRACE and Envisat satellite missions, respectively. Using empirical orthogonal functions and singular value decompositions of each data set, we find a quasi 4.7-yr periodic signal between 08/2002 and 10/2010 that accounts for ∼15–30% of the time variability of the filtered and detrended surface-mass and elevation data. Computation of the density of this variable mass load corresponds to snow or uncompacted firn. Changes reach maximum amplitude within the first 100 km from the coast where it contributes up to 30–35% of the annual rate of accumulation. Extending the analysis to 09/2014 using surface-mass changes only, we have found anomalies with a periodicity of about 4–6 yrs that circle the AIS in about 9–10 yrs. These properties connect the observed anomalies to the Antarctic Circumpolar Wave (ACW) which is known to affect several key climate variables, including precipitation. It suggests that variability in the surface-mass balance of the Antarctic Ice Sheet may also be modulated by the ACW.

1. Introduction

As revealed by analyzing linear trends in surface-height variations estimated from radar altimetry data of the ERS (1992–2003) and Envisat (2002–2006) satellites (Rémy and Parouty, 2009), the elevation of the Antarctic Ice Sheet (AIS) is subject to decimetric scale variability over periods of a few years. Using satellite altimetry and gravimetry data, Mémin et al. (2014) have obtained a map for the rates of snow-height changes in the AIS that shows a regional pattern along the coast that may be driven by interannual variability in accumulation. Analysis of surface-mass and elevation changes over the AIS, as observed by satellite gravimetry and altimetry, respectively, has already been used to quantify the spatial distribution of rates of snow- and ice-mass change in Antarctica (e.g. Gunter et al., 2009; Lee et al., 2012; Mémin et al., 2014). Characterizing the interannual signal within these data will help to further quantify variability in surface-mass balance across the AIS and thus assist with understanding its origin (Sasgen et al., 2010; Horwath et al., 2012; Boening et al., 2012).

Our aim is to investigate the interannual changes in the mass redistribution over the AIS using a combined analysis of surface-mass and elevation variations. We apply singular value decomposition (SVD) and empirical orthogonal function (EOF) methods to satellite gravimetry and altimetry data in Section 2. Results are analyzed in Section 3 while we discuss the changing mass over the AIS in Section 4. Conclusions follow in Section 5.

2. Surface-mass and elevation time series

The Gravity Recovery and Climate Experiment (GRACE) satellite mission provides with the space–time variability of the Earth's gravity field since April 2002 (Tapley et al., 2004). We use Stokes coefficients up to degree/order 50 of the release 5 of the Center for Space Research (CSR) solutions. We replace the degree-2 zonal harmonic with Satellite Laser Ranging (SLR) estimates (Cheng et al., 2013) and compute monthly changes of surface-mass applying a Gaussian averaging function with a 300-km radius (Jekeli, 1981; Wahr et al., 1998). We use Envisat altimetric

* Corresponding author.
E-mail address: anthony.memin@geoazur.unice.fr (A. Mémin).

http://dx.doi.org/10.1016/j.epsl.2015.03.045
0012-821X/

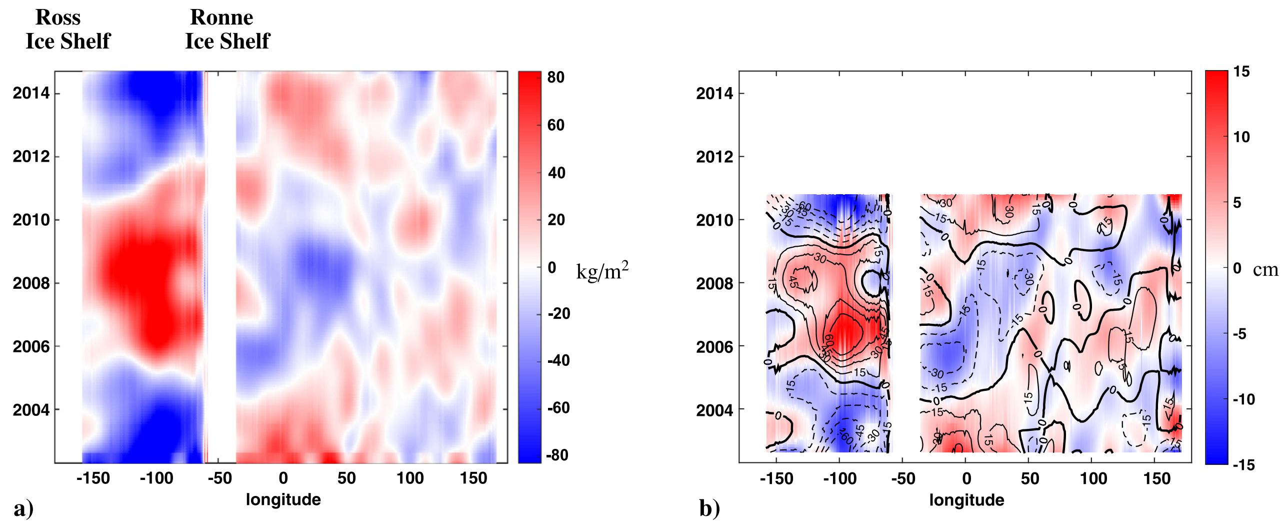

Fig. 1. Time–longitude diagrams of a) surface-mass changes between 04/2002 and 09/2014 and b) elevation (background color, in cm) and surface-mass (contour lines, in kg/m^2) changes during Envisat period (08/2002–10/2010). Longitude values are temporal meridional averages. A degree-1 polynomial is removed from the initial time series and according to the time interval considered. The solid and dash contour lines are for positive and negative values, respectively. (For interpretation of the references to color in this figure legend, the reader is referred to the web version of this article.)

data as Mémin et al. (2014). A detailed description of the processing strategy is provided by Flament and Rémy (2012) and Mémin et al. (2014, supplementary material). We estimate 98 monthly maps of spatial changes of elevation of the AIS between August 2002 and October 2010 and 138 of surface mass between April 2002 and September 2014. Monthly variations are computed with respect to March 2004 as it is the first Envisat cycle with the most complete coverage.

Envisat data yield elevation changes with higher spatial resolution (5 km) compared to surface-mass changes estimated from GRACE solutions (400 km). To compare both fields, we reduce the spatial resolution of the monthly maps of the AIS elevation change by applying a GRACE-like processing approach as outlined by Mémin et al. (2014). Monthly maps of surface-mass and elevation changes are finally output on $1^\circ \times 1^\circ$ grids providing 2959 time series for each field located North of 81.5°S due to the inclination of the Envisat orbit and thus the limited coverage of the surface elevation data.

To focus on the interannual signal we apply a low-pass Vondrak filter to each individual time series to remove signals containing high-frequency noise and seasonal variability. Since we are not interested in the long-term trend that can be related to present-day ice-mass changes or glacial isostatic adjustment induced by past ice-mass changes (e.g. King et al., 2012; Shepherd et al., 2012), we further remove a linear trend estimated by using the least-squares method.

We show in Figs. 1-a and 1-b time–longitude diagrams, also known as Hovmöller diagram (Hovmöller, 1949), obtained by computing meridional averages over the AIS of monthly surface-mass and elevation variations, respectively. In Fig. 1-b, the contour lines correspond to averages of surface-mass variations detrended on the same time interval as the elevation variations. Besides the noticeable agreement between these two fields from 08/2002 to 10/2010, we can see anomalies propagating eastward. The propagation pattern is also revealed in surface-mass variations between 04/2002 and 09/2014, even though amplitudes have changed, mostly in the West.

To analyze the interannual variability over Antarctica we apply the EOF method on each individual field and perform an SVD of the two fields simultaneously on the common time interval. EOF and SVD are powerful methods to analyze spatio-temporal variabilities of one and two data sets, respectively. For example, both methods have been successfully applied on Sea Surface Temperature (SST) and Sea Level Pressure (SLP) in the Persian Gulf to show a strong atmosphere–ocean coupling (Hassanzadeh et al., 2007). EOF and SVD methods are well-described in the literature (e.g. Björnsson and Venegas, 1997; Hassanzadeh et al., 2007). Applying either method we obtain 1) expansion coefficients that represent modes of temporal variability; 2) spatial coefficients that weight each mode; and 3) measures of the significance of the modes. The latter are expressed as the percentage of explained variance (EOF) or squared covariance fraction (SCF, SVD). SVD further provides with coupled space and time variations of the two fields.

Table 1
Squared Covariance Fraction (SCF) and variance (Var.) statistics (Stat.) obtained from the SVD and EOF analyzes of surface-mass ($\Delta\sigma$) and elevation (Δh) changes estimated from GRACE and Envisat data, respectively. Analyzes are performed over a time interval of 8.2 (^{a}) and 12.4 (^{b}) yrs. For the latter, figures (^{c}) associated with the mode 3 have been replaced by those for the mode 4 as detailed in the text. Unit: %.

Modes		1	2	3	1+2+3
Parameter	Method/Stat.				
Δh^a, $\Delta\sigma^a$	SVD/SCF	65.3	18.3	6.6	90.2
Δh^a	EOF/Var.	55.1	20.9	10.7	86.7
$\Delta\sigma^a$	EOF/Var.	72.7	15.7	4.7	93.1
$\Delta\sigma^b$	EOF/Var.	83.0	5.8	2.1^c	90.9^c

3. Analysis of the AIS interannual signal

Between 08/2002 and 10/2010, the three leading EOF modes explain more than 93 and 86% of the filtered surface-mass and elevation changes, respectively (Table 1). More than 72 and 55% of the variability in surface-mass and elevation changes is due to the first mode, while together the second and third modes account for more than 20 and 31%, respectively. There is a very good agreement between the expansion coefficients obtained for surface-mass changes and that obtained for elevation changes with coefficients of correlation of about 0.99, 0.95 and 0.67 for the leading mode 1, 2 and 3, respectively (Fig. 2). The expansion coefficients of the three leading modes obtained with the SVD method are highly correlated (≥ 0.91) to that obtained with EOFs. This indicates that surface-mass and elevation changes are strongly coupled for these modes and that the coupled signals account for a large fraction of the observed variability. Indeed, the three leading SVD modes explain 90% of the SCF (65% for the first mode and 25% for the second and third modes).